Journal of Power Sources 213 (2012) 83–92

Contents lists available at SciVerse ScienceDirect

Journal of Power Sources

journal homepage: www.elsevier.com/locate/jpowsour

Sulfonated poly(ether ether ketone)/amino-acid functionalized titania hybrid proton conductive membranes

Hong Wu [a,b], Xiaohui Shen [a], Tao Xu [a], Weiqiang Hou [a], Zhongyi Jiang [a,*]

[a] *Key Laboratory for Green Chemical Technology, School of Chemical Engineering and Technology, Tianjin University, Tianjin 300072, China*
[b] *Tianjin Key Laboratory of Membrane Science and Desalination Technology, Tianjin University, Tianjin 300072, China*

ARTICLE INFO

Article history:
Received 26 January 2012
Received in revised form
1 April 2012
Accepted 3 April 2012
Available online 19 April 2012

Keywords:
Titania submicrospheres
Sulfonated poly(ether ether ketone)
Hybrid membranes
Methanol permeability
Proton conductivity
Direct methanol fuel cell

ABSTRACT

Inspired by the proton conducting mechanism in organisms where the amino acid groups play a crucial and multiple role, a novel kind of amino acid-functionalized titania submicrospheres was prepared and incorporated into sulfonated poly(ether ether ketone) (SPEEK) to fabricate the hybrid membranes for potential application in direct methanol fuel cells (DMFCs). The pristine titania submicrospheres (TiO_2) with a uniform particle size of ~220 nm were synthesized via a sol–gel process and modified with amino acid groups through a facile chelation method. Meanwhile, amino groups, carboxylic groups and phenyl groups were introduced in the same way for comparison purpose. Compared with the control SPEEK membrane, the methanol crossover was reduced and the membrane mechanical strength was enhanced by incorporation of the functionalized titania submicrospheres. Due to the different proton acceptor/donor capability of the different functional groups, the hybrid membrane embedded with amino-functionalized titania exhibited lower proton conductivity at 20 °C but higher values at elevated temperature of 60 °C compared with carboxylic-functionalized titania; the hybrid membrane embedded with amino acid-functionalized titania displayed a superior proton-conducting ability with the highest proton conductivity of 0.258 S cm^{-1} at 60 °C.

1. Introduction

Proton exchange membranes (PEMs) are the key component in the development of direct methanol fuel cells (DMFCs) [1,2]. However, the profound drawbacks of current PEMs (e.g. Nafion®), such as serious methanol crossover, reduced proton conductivity at high temperature and high cost, have impeded the wide commercial application of DMFCs [3,4].

To address this issue, one commonly utilized candidate is the hybrid membranes which have the potential to provide unique combinations of organic and inorganic moieties [5]. However, the presence of inorganic fillers (e.g. montmorillonite [6], titanium oxide [7], zeolite [8], silica [9] and zirconium oxide [10]) usually reduces the proton conductivity due to their intrinsically low proton conductivity and consequently considerable dilution effect of acid concentration in the original polymer matrix [9]. Therefore, functionalization of inorganic fillers with proton-conducting groups is widely adopted to minimize the loss of proton conductivity [11]. It has been demonstrated that incorporating acid groups, mainly including the sulfonic acid groups [6,12–14], phosphonic acid groups [15,16] and carboxylic acid groups [17], can increase the ion-exchange capacity (IEC), the amount of active proton conducting sites and water content, thus improving the proton conductivity of the membrane. In our previous studies, titania submicrospheres grafted with phosphonic acid [16] and sulfonic acid groups [18] were blended into chitosan and SPEEK respectively to improve the proton conductivity of the hybrid membranes. It has also been found that the effect of the filler on the properties of the composite membranes strongly depends on the nature of polymer matrix. The conductivities of the chitosan/phosphonic acid-modified titania membrane and the SPEEK/sulfonic acid-modified titania membrane were 0.011 and 0.053 S/cm, respectively, both higher than their respective control membranes. Guiver et al. [14] reported a 3.6-fold increase of proton conductivity of SPEEK membrane after embedding 7.5 wt.% of sulfonated silica nanoparticles. Davis and co-workers [17] synthesized carboxylic acid groups within MCM-41 to enhance proton conductivity. The generated nonporous proton-conducting solid acid displayed a moderate conductivity of 6 mS cm^{-1} at 95 °C, a quite promising alternative for PEMs in DMFCs. Moreover, basic groups such as amino groups [19–21] and nitrogen heterocycles [22] are also

---

* Corresponding author. Tel./fax: +86 022 23500086.
E-mail address: zhyjiang@tju.edu.cn (Z. Jiang).

0378-7753/$ – see front matter © 2012 Elsevier B.V. All rights reserved.
doi:10.1016/j.jpowsour.2012.04.003

utilized as pendent chains to enhance the proton conductivity at elevated temperature. The enhancement in conductivity is mainly attributed to more bound water interacting with the nitrogenous base by forming hydrogen bridges as well as protonation of the nitrogen sites [21]. Chen et al. [20] synthesized poly(oxyalkylene) diamine-functionalized carbon nanotube (CNT)/Nafion nanocomposites and postulated that these closely assembled amino-bearing chains facilitated proton transportation by the binding of water as well as the $-NH_3^+SO_3^-$− ionic pathway for proton transfer along the carbon nanotube wall. This approach provided continuous paths to facilitate proton conduction ($\sigma = 2.8 \times 10^{-2}$ S cm^{-1} at 30 °C; $\sigma = 6.3 \times 10^{-2}$ S cm^{-1} at 130 °C). However, there are few reports on utilization of amino acid groups in fabricating proton exchange membranes.

It is well known that amino acids play a vital role in the proton-transfer process in biology, represented by cytochrome complex [23] and bacteriorhodopsin [24,25], where proton transfer occurs along amino acid-lined channels and each amino acid acts simultaneously as both a proton donor and a proton acceptor. Intrigued by this, Tributschet al. [26] utilized the electrostatic interactions to attach amino acids (L-lysine, aspartic acid, methionin) to silica nanoparticles which were then incorporated into porous membranes (PET, PC) with pores between 100 and 400 nm to fabricate amino acid-modified membranes. The power output of such membrane was of a similar order of magnitude as that for Nafion®. However, anchoring the amino acids firmly within the membrane remains one of the key technical challenges. Fortunately, mussel-inspired bioadhesion devotes an excellent approach to deal with this challenge. It is well known that catechol and catecholic derivatives with various functional groups could readily chelate with transition metal (Ti, Zr etc.) to form a stable metal-catecholic salt complex, thus being covalently grafted on almost any available transition metal surface under mild conditions [27–30].

In this study, four kinds of functionalized titania submicrospheres were incorporated into sulfonated poly(ether ether ketone) (SPEEK) to fabricate the hybrid membranes for potential application in direct methanol fuel cells (DMFCs). The pristine titania submicrospheres (TiO_2) were synthesized via a sol–gel process and modified respectively with dopa, dopamine, catechol and 3-(3,4-dihydroxyphenyl) propionic acid through a facile chelation method to endow the titania surface with four different kinds of functional groups including amino acid groups, amino groups, carboxylic groups and phenyl groups. The functionalized titania submicrospheres were characterized by TEM, FTIR and XPS and the hybrid membranes were characterized by FTIR and FESEM. Membrane properties were assessed in terms of thermal stability, ionic exchange capacity (IEC), swelling behavior, proton conductivity and methanol permeability.

2. Experiment

2.1. Materials and chemicals

Poly(ether ether ketone) (PEEK) was purchased from Victrex High-performance Materials (Shanghai, China) Co., Ltd. 3-(3,4-dihydroxyphenyl) propionic acid was purchased from Alfa Aesar. 3-(3,4-dihydroxyphenyl)-L-alanine (L-Dopa) and 2-(3,4-dihydroxyphenyl) ethylamine (Dopamine)were purchased from Yuancheng Technology Development Co., Ltd. (Wuhan, China). Catechol, tetrabutyl titanate (TBT, >98%) and ethylene glycol were purchased from Tianjin Guangfu Fine Chemical Research Institute (Tianjin, China). N,N-dimethylformamide (DMF), sulfuric acid, acetone and methanol were of analytical grade and purchased locally.

Sulfonated poly(ether ether ketone) (SPEEK)with a sulfonation degree of 67% was prepared by direct sulfonation of PEEK [31]. PEEK was firstly dried in oven at 80 °C for 24 h before sulfonation. Then, the dried PEEK (14 g) was gradually dissolved into 100 mL sulfuric acid (H_2SO_4, 95–98%) in a three-neck flask for about 3 h at room temperature, followed by vigorous stirring at 45 °C for 8 h. Afterward, the polymer solution was gradually precipitated into ice-cold water under mechanical agitation. Finally, the polymer precipitate was filtered, washed several times with de-ionized water until pH reached neutral and then dried first at room temperature for 24 h and then at 60 °C for another 24 h. The sulfonation degree (DS) was determined to be 67% through acid–base titration method [32].

2.2. Preparation of functionalized titania submicrospheres

Titania submicrospheres (TiO_2) with a particle size of about 220 nm were synthesized by sol–gel method as described in previous study [33]. For modifying titania, L-dopa, dopamine, catechol and 3-(3,4-dihydroxyphenyl) propionic acid (molecular structures shown in Scheme 1) were used as modification reagents. A facile chelation procedure was conducted. A certain amount of TiO_2 powders was suspended in hydrochloric acid aqueous solution (pH = 2) under ultrasonic treatment for 2 h to break aggregates. The obtained solution was poured into a large excessive 4 mg mL^{-1} modification reagent solution (pH = 2), followed by vigorous stirring for 30 min. The functionalized titania submicrospheres were collected by centrifugation, washed with distilled water until neutral and dried in a vacuum oven at 80 °C for 24 h. The final obtained functional titania submicrospheres grafted with amino groups ($-NH_2$), carboxylic groups ($-COOH$), phenyl groups ($-Ph$) and amino acid groups were designated as TiO_2–N, TiO_2–C, TiO_2–P and TiO_2–NC, respectively. The chemisorption process of catecholic salt on the titania reached equilibrium within 10 min and the low pH prevented the catechol end groups of the reagents from oxidation [28,29].

2.3. Membrane preparation

SPEEK (1.2 g) was dissolved in 8 g DMF at room temperature. A measured amount of functionalized titania submicrospheres were dispersed in 4 g DMF and the resulting suspension was added into SPEEK-DMF solution under vigorously stirring for 24 h to get a fine dispersion of inorganic particles in the polymer solution. After degasification, the mixture was poured onto a clean glass plate and heated overnight in an oven at 60 °C for 12 h, followed by annealing at 80 °C for another 12 h. The membranes were peeled off from the glass plate, followed by immersion in 1 M HCl solution for 48 h and subsequently rinsing with de-ionized water several times to

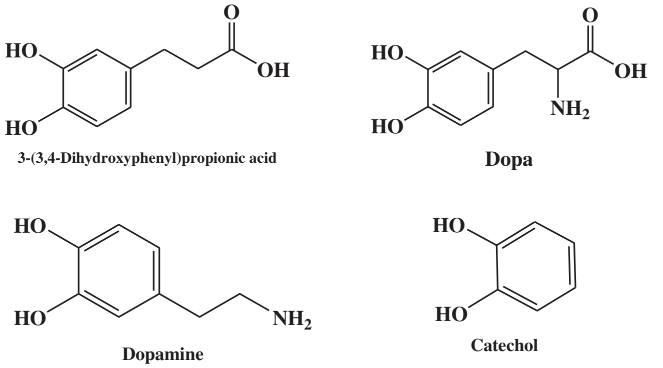

Scheme 1. The molecular structures of the modification reagents.

remove residual acid. The as-prepared membranes were then dried under vacuum at 25 °C for 24 h and designated as SPEEK/TiO_2–X, SPEEK/TiO_2–C–X, SPEEK/TiO_2–N–X, SPEEK/TiO_2–P–X and SPEEK/TiO_2–NC–X, where TiO_2, TiO_2–C, TiO_2–N, TiO_2–P, TiO_2–NC represented the inorganic fillers and X (= 5, 10, 15 or 20) was the weight ratio percentage of fillers to SPEEK. The pure SPEEK membrane was also fabricated as control membrane. The thickness of the as-prepared membranes was in the range of 55–70 μm.

2.4. Characterizations

The morphology of the titania submicrospheres was characterized by transmission electron microscopy (TEM). The cross-sectional morphologies of the membranes were observed using field emission scanning electron microscope (FESEM, Nanosem 430) operated at 15 kV. The cross-sections were prepared by freeze-fracturing in liquid nitrogen and subsequently coated with a thin layer of sputtered gold.

The surface chemical composition of the titania submicrospheres was monitored by X-ray photoelectron spectroscopy (XPS) using a PHI 1600 spectrometer with Mg Kα radiation for excitation. Fourier transform infrared spectra (FTIR, 4000–400 cm^{-1}) were recorded on a Nicolet MAGNA-IR 560 instrument.

Thermogravimetric analysis (TGA) was performed using a thermogravimetric analyzer (Perkin–Elmer Pyris) over a temperature range of 20–800 °C at a heating rate of 10 °C min^{-1}under nitrogen flow. Each sample was vacuum-dried at 100 °C for 24 h prior to measurement to remove absorbed water.

Mechanical property test of the membranes was conducted using an Instron Mechanical Tester (Testometric 350 AX). Each sample was cut into 1.0 cm × 4.0 cm and examined with an elongation rate of 4 mm min^{-1} at room temperature.

2.5. Dimensional swelling

The dimensional swelling degree of the membrane was measured. A piece of dry, rectangular-shaped membrane sample (4.0 cm × 4.0 cm) with an area of A_{dry} (cm^2) was soaked in water at 25, 30, 35, 40 and 45 °C for 12 h to allow full hydration and then re-measured (A_{wet}, cm^2). The dimensional swelling degree was the average of two measurements with an error within ±3.0%.

$$\text{Swelling degree}(\%) = \frac{A_{wet} - A_{dry}}{A_{dry}} \times 100\% \quad (1)$$

2.6. Ion-exchange capacity (IEC)

The IEC value of the membrane was measured using a classical back titration method at room temperature. The membrane in acidic form was equilibrated in 2 M NaCl solution for 48 h to replace H^+ ions by Na^+ ions completely. Released protons were then titrated with 0.01 M NaOH aqueous solution using phenolphthalein as indicator. The IEC value was calculated by Eq. (2),

$$\text{IEC}\left(\text{mmol g}^{-1}\right) = \frac{0.01 \times 1000 \times V_{NaOH}}{W_d} \quad (2)$$

where V_{NaOH} (L) was the volume of NaOH solution consumed for titration and W_d (g) was the weight of the dry membrane sample. The measurements were carried out with an accuracy of 0.001 mmol g^{-1}.

2.7. Methanol permeability, proton conductivity and selectivity

The methanol permeability of the membrane was measured at room temperature using a glass diffusion cell [32] which consisted of two compartments of identical volume. The membrane was fully hydrated in water before being clamped tightly between the two compartments, one of which was filled with 2 M methanol solution and the other filled with water. The methanol concentration in the water compartment was analyzed periodically by a gas chromatography (Agilent 6820) equipped with a thermal conductivity detector (TCD) and a DB624 column. The methanol permeability (P, cm^2 s^{-1}) was calculated by Eq. (3),

$$P = S\frac{V_B l}{AC_{A0}} \quad (3)$$

where S was the slope of the straight line of concentration versus time, V_B was the volume of the receipt compartment, and l, A, and C_{A0} were the membrane thickness, effective membrane area and feed concentration, respectively. Three repeated measurements were conducted and the standard deviations were ±4.0%.

The proton conductivity of the membranes in transverse direction was measured by a two-point-probe method using an impedance analyzer. The membrane impedance was measured using a frequency response analyzer (FRA, Compactstat, IVIUM Tech.) over a frequency range of 1–10^6 Hz with oscillating voltage of 20 mV. The membrane sample was first soaked in distilled water for 24 h prior to conductivity measurement to ensure full hydration. Then, the sample was put into the cell and heated by water vapor at a certain temperature ranging from 20 to 85 °C. The relative humidity was kept at 100% during test. The sample was kept in the saturated water vapor for a certain period of time and the conductivity was monitored until constant value. The proton conductivity (σ, S cm^{-1}) of the samples was calculated according to the following Eq. (4),

$$\sigma = \frac{l_0}{AR} \quad (4)$$

where l_0 and A were the distance between the two electrodes and the cross-sectional area of the membrane, respectively, and R was the membrane resistance derived from the low intersection of the high frequency semicircle on a complex impedance plane with Re (z) axis. Three repeated measurements were conducted and the standard deviations were ±5.0%.

The overall membrane characteristic was expressed in terms of selectivity (β) defined as the ratio of proton conductivity to methanol permeability [34],

$$\beta = \frac{\sigma}{P} \quad (5)$$

3. Results and discussion

3.1. Characterizations of the titania submicrospheres

Fig. 1(a) showed the TEM image of the titania submicrospheres. The as-synthesized titania submicrospheres were morphologically identical and monodispersed with an average particle size of approximately 220 nm Fig. 1(b–f) showed the photographs of the titania powder before and after modification. A color change from white (TiO_2) to brown (TiO_2–C, TiO_2–N, TiO_2–NC) or dark gray (TiO_2–P) could be clearly observed upon contacting with the modification reagents.

FTIR and XPS were employed to elucidate the surface composition of these functionalized titania submicrospheres. As shown in Fig. 2(a), compared with the spectrum of pristine titania, the characteristic peaks of ethylene glycolon the pristine titania surface at 1080, 2868 and 2930 cm^{-1} [16] disappeared after modification and the corresponding characteristic absorption bands (1000–1750 cm^{-1}) of the functional groups appeared. This could be as an indication of successful functionalization.

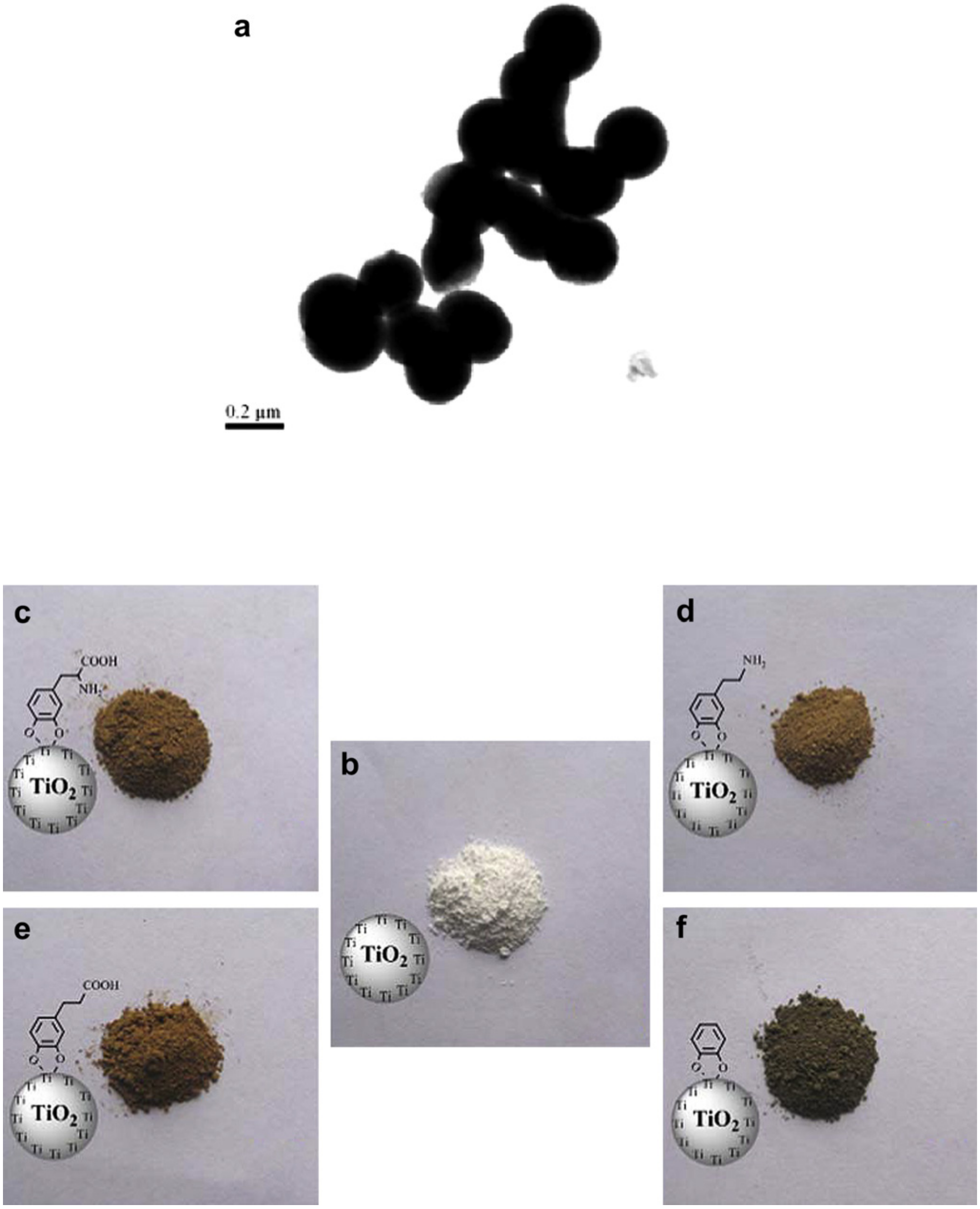

Fig. 1. TEM image of TiO_2 submicrospheres (a); photograph of the as-synthesized $TiO_2$and the functional TiO_2 powders: TiO_2 (b), TiO_2–NC (c), TiO_2–N (d), TiO_2–C (e), TiO_2–P (f).

The XPS spectra of the functionalized titania and the pure sample were shown in Fig. 2(b). For pristine titania, a strong peak at 532.2 eV and a weak peak at 529.8 eV were detected, attributing to the oxygen atom in C–O–Ti bond and Ti–O–Ti bond, respectively. This result indicated that ethylene glycol was attached to the titania surface via formation of C–O–Ti covalent bonds. As for the functionalized titania (TiO_2–N and TiO_2–NC), the relatively strong peak corresponding to the oxygen in the C–O–Ti bond shifted to a lower binding energy (532.0 eV) by 0.2 eV. This result provided an additional evidence of the successful chelation process. Based on the above analysis, the amino acid functionalization process was depicted in Fig. 2(c) as an example.

3.2. Characterizations of the membranes

The membrane morphologies were investigated by examining the fracture surface using FESEM. Fig. 3 exhibited the cross-section images of the control SPEEK membrane and the SPEEK/TiO_2–NC hybrid membranes with TiO_2–NC content of 5, 10, 15 and 20 wt.%. The morphologies of the other three kinds of hybrid membranes containing TiO_2–N, TiO_2–C and TiO_2–P were similar with those shown in Fig. 3. These images indicated that the membranes were relatively dense without any apparent defect and the inorganic particles dispersed homogeneously within the membrane. As for SPEEK/TiO_2–NC, SPEEK/TiO_2–C and SPEEK/TiO_2–N membranes, the fine dispersion was mainly attributed to the hydrogen bonding interactions between the functionalized titania fillers and polymer bulk matrix as well as the electrostatic repulsive force among particles with the same surface charge. With respect to the SPEEK/TiO_2–P membrane, the fine dispersion was mainly originated from the weak attractive van der Waals forces among titania particles [35].

The FTIR spectra of the SPEEK control membrane and the SPEEK/TiO_2–NC hybrid membranes were shown in Fig. 4. The absorption bands at 1020, 1080 and 1253 cm^{-1} were assigned to the asymmetric and symmetric stretching vibrations of O=S=O [36]. After incorporating titania submicrospheres, the intensity of the

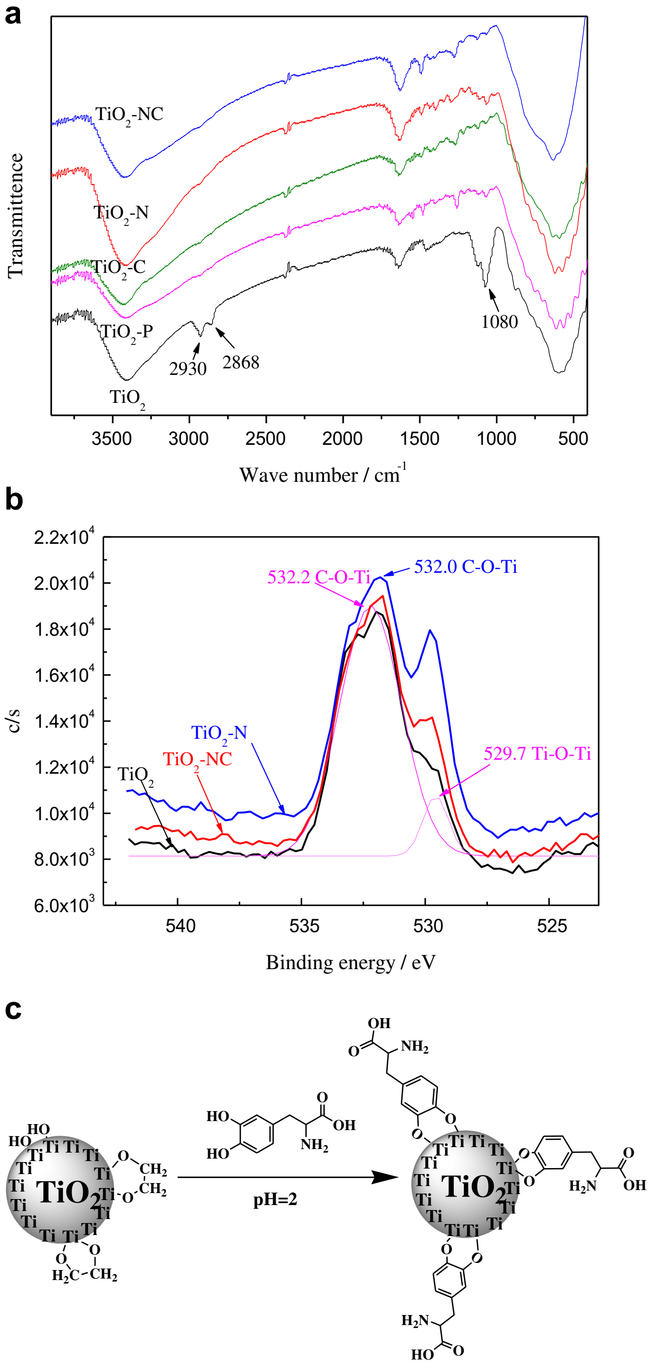

Fig. 2. FTIR spectra (a) and XPS spectra of O 1 s (b) of TiO_2–NC and TiO_2; amino acid functionalization of TiO_2 (c).

characteristic peaks of $-SO_3H$ group decreased as the content of the filler increased from 0 to 20 wt.%. Such observations were reasonably derived from the formation of interfacial interactions including the hydrogen bonds and electrostatic force between the TiO_2–NC and the SPEEK polymer.

3.3. Thermal and mechanical stabilities of the hybrid membranes

Good thermal and mechanical properties are crucial for the proton exchange membrane in DMFCs to guarantee a long lifetime of the fuel cells [12]. The thermal properties of the membranes were investigated by thermogravimetry programmed from 30 to 700 °C as shown in Fig. 5(a). All the membranes exhibited three major weight loss stages. The initial weight loss around 150 °C was attributed to the evaporation of adsorbed water and residual solvent. The weight loss region starting from about 290 °C could be ascribed to the decomposition of the $-SO_3H$ groups [31,32], and then followed by the weight loss from the degradation of the polymer main chains at about 490 °C. No obvious shift in the onset decomposition temperature of the sulfonic acid group was observed, which might be due to the low content of the filler. A relatively lower degradation temperature for membranes embedded with functional fillers was observed in the last two weight loss stages, mainly due to the degradation of the organic parts grafted on the titania surface. The hybrid membranes displayed good thermal stability below 300 °C, sufficiently for practical applications in DMFCs.

Fig. 5(b) presented the mechanical strength characterization of the control SPEEK and the hybrid membranes with the same content (15 wt.%) of various functionalized titania fillers. The control SPEEK membrane displayed good ductility with a tensile strength of 42 MPa and an elongation at break of 160%. Due to the rigidity of the inorganic fillers, which could restrict the polymer chain segmental mobility and enhance the rigidity of resultant hybrid membranes [12], the degree of elongations for the hybrid membranes were remarkably decreased to about 110% while the Tensile strength increased. The SPEEK/TiO_2–N membrane displayed the maximum Tensile strength value of about 52 MPa, which was mainly ascribed to the strong acid–base interaction between SPEEK and TiO_2–N.

3.4. Swelling behavior of the hybrid membranes

The dimensional swelling degrees of the SPEEK and hybrid membranes at different temperatures were measured and displayed in Fig. 6. The dimensional swelling degree increased with increasing temperature. Compared with the control SPEEK membrane, the dimensional swelling degrees of the hybrid membranes were notably reduced by the incorporation of inorganic titania fillers (Fig. 6(a)). With the increase of TiO_2–NC content in the membrane, the dimensional swelling of the hybrid membrane was repressed (Fig. 6(b)). This result indicated that incorporation of the inorganic fillers was propitious to the membrane size stability. Besides, at the same fillers content, the swelling degrees of the SPEEK/TiO_2–NC and SPEEK/TiO_2–N hybrid membranes were slightly lower than that of SPEEK/TiO_2 hybrid membrane. Incorporation of TiO_2–NC or TiO_2–N particles into SPEEK polymer matrix resulted in extensive interaction between the surface groups of the particles and the sulfonic acid groups of the polymer, thus reducing the swelling degree of the membrane [37].

3.5. Ion-exchange capacity

The ion-exchange capacity (IEC) values of the resultant membranes were presented in Table 1. Regardless of the various kinds of functionalized titania fillers, the measured IEC values of the hybrid membranes were found to be lower than that of the plain SPEEK membrane (IEC = 1.93 mmol g^{-1}, DS = 67%). The addition of inorganic fillers into SPEEK matrix exerted a dilution effect on the concentration of the strongly acidic sulfonic group in the membrane and thus decreased the IEC values [9,16]. The higher the amount of inorganic fillers added in the hybrid membrane, the lower the IEC values. Furthermore, thanks to the partial compensation effect of the amino acid groups and carboxylic acid groups, the IEC values of SPEEK/TiO_2–NC (1.73–1.86 mmol g^{-1}) and SPEEK/TiO_2–C (1.78 mmol g^{-1}) hybrid membranes were higher than or

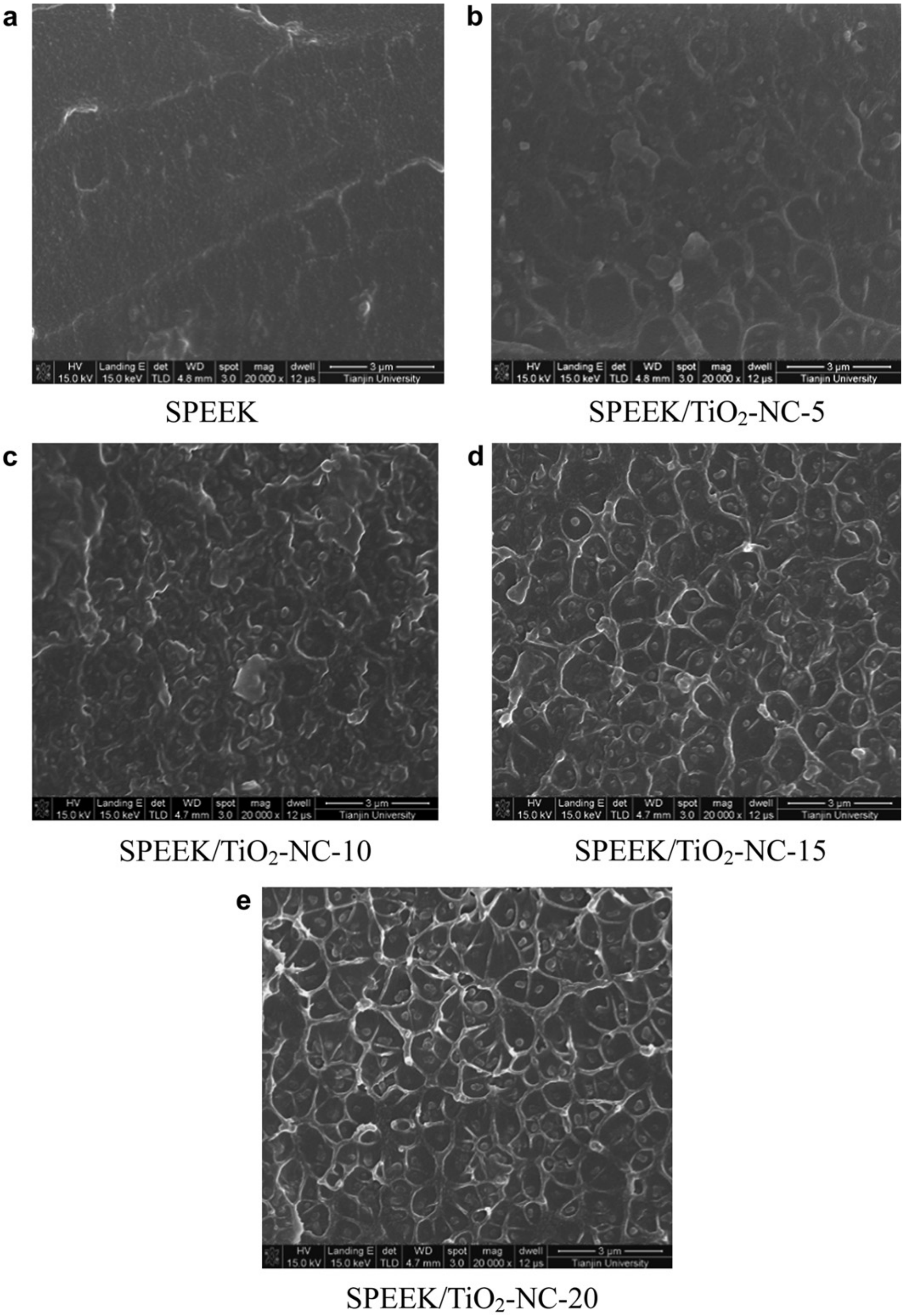

SPEEK

SPEEK/TiO_2-NC-5

SPEEK/TiO_2-NC-10

SPEEK/TiO_2-NC-15

SPEEK/TiO_2-NC-20

Fig. 3. FESEM images of the cross-section of SPEEK and SPEEK/TiO_2–NC hybrid membranes: SPEEK (a), SPEEK/TiO_2–NC–5 (b), SPEEK/TiO_2–NC–10 (c), SPEEK/TiO_2–NC–15 (d), SPEEK/TiO_2–NC–20 (e).

comparable with that of the membrane doping with pure titania submicrospheres (1.78 mmol g^{-1}).

3.6. *Proton conductivity*

The proton conductivity of the membranes measured at room temperature at 100% RH was listed in Table 1. Accordingly, the conductivity of the as-prepared membranes with an identical filler content of 15 wt.% increased in the following order: SPEEK/TiO_2–C–15 (0.071 S cm^{-1}) > SPEEK/TiO_2–NC–15 (0.066 S cm^{-1}) > SPEEK (0.051 S cm^{-1}) > SPEEK/TiO_2–N–15 (0.047 S cm^{-1}) > SPEEK/TiO_2–P–15 (0.043 S cm^{-1}) > SPEEK/TiO_2–15 (0.039 S cm^{-1}). The pure SPEEK membrane exhibited an adequate proton conductivity for DMFC applications (>0.01 S cm^{-1}). Addition of pristine titania into the

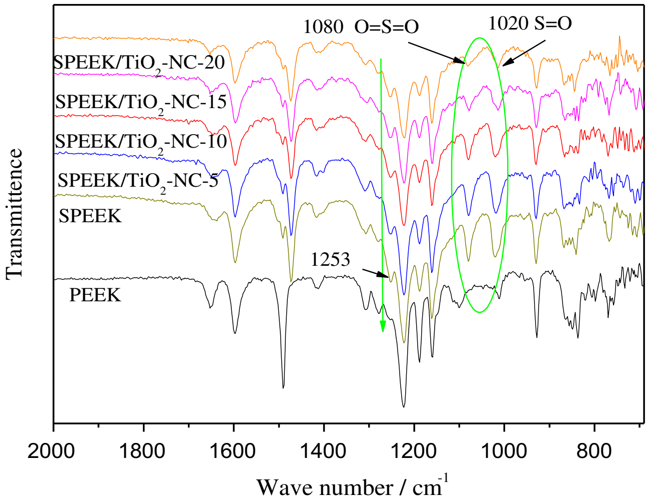

Fig. 4. FTIR spectra of PEEK, SPEEK and hybrid membranes.

SPEEK matrix resulted in a reduction in sulfonic acid group concentration and thus lowering the membrane's proton conductivity. Modification of the titania surface with amino groups and phenyl groups improved the proton conducing property to some extent due to the improved compatibility between the polymer matrix and the inorganic fillers. Incorporation of carboxyl acid-functionalized and amino acid-functionalized titania led to a remarkable increase in proton conductivity which was higher than both the pure SPEEK membrane and the SPEEK/TiO_2 membrane. It was reasonable to believe that these various functional groups grafted on the inorganic titania particles exerted different influences on the proton transfer in the membrane.

Generally, proton transport mechanisms through a PEM principally involve the vehicle mechanism (the protons diffuse together with water molecules by forming complexes) and Grotthuss mechanism (the protons jump via rearrangement of proton convey sites through hydrogen bonds) [38,39]. Herein, the addition of titania grafted by hydrophilic groups (amino acid groups, carboxylic acid groups and amino groups) into the polymer matrix rendered an increasing amount of absorbed water molecules which tended to form more continuous hydrophilic pathways to facilitate the proton transport by vehicle mechanism. Furthermore, the homogeneously dispersed TiO_2–C and TiO_2–NC within the SPEEK matrix would open a new avenue for proton migration with the aid of the functional surface acidic groups as well as the adsorbed water, thus facilitating the proton transport according to the Grotthuss mechanism [40–42]. As to amino-functionalized titania (SPEEK/TiO_2–N), numerous sulfonic acid groups on the SPEEK

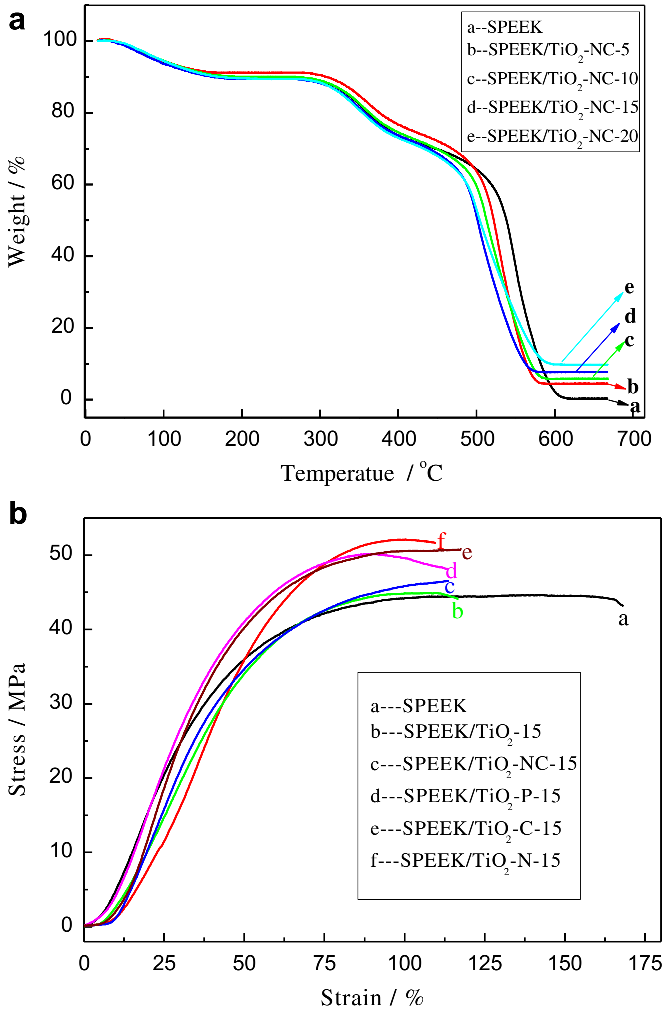

Fig. 5. TGA curves (a) and stress–strain curves (b) of SPEEK and hybrid membranes.

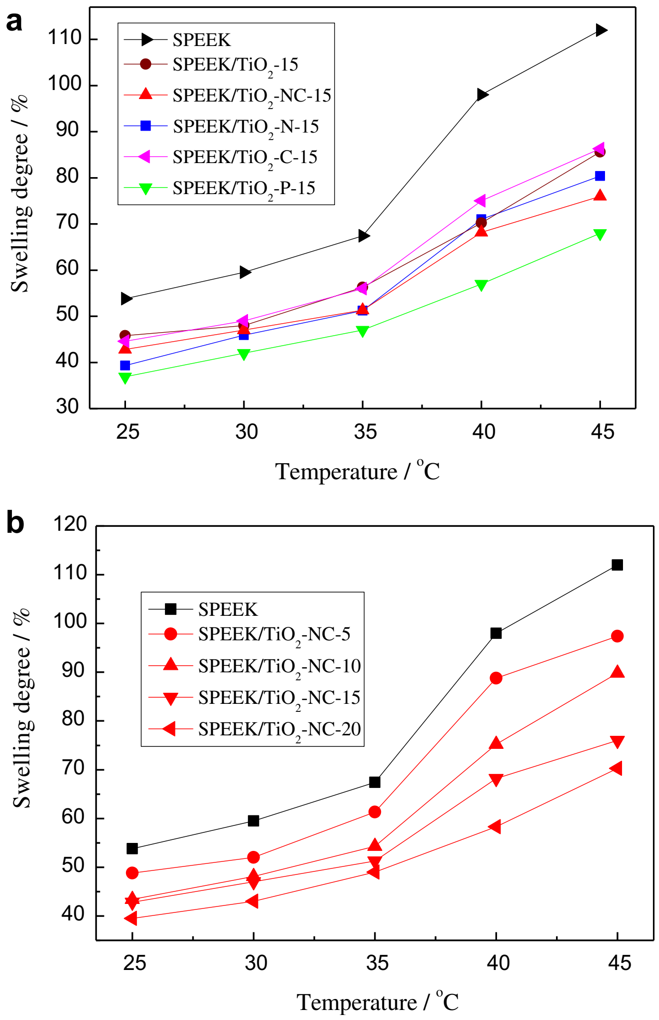

Fig. 6. Dimensional swelling degree of SPEEK and hybrid membranes at different temperatures with various functional fillers (a) and different filler contents (b).

Table 1
IEC, proton conductivity, methanol permeability and selectivity of the membranes at room temperature.

Membrane	IEC (mmol g^{-1})	σ (S cm^{-1})[a] 20 °C	P ($\times$ $10^{-7}$$cm^2s^{-1}$)[b]	β ($\times$ 10^4 S s cm^{-3})
			2 M methanol	20 °C, 2 M methanol
SPEEK	1.93	0.051	11.70	4.39
SPEEK/TiO_2–15	1.78	0.039	8.44	4.62
SPEEK/TiO_2–NC–5	1.86	0.056	9.54	5.87
SPEEK/TiO_2–NC–10	1.84	0.060	8.51	7.05
SPEEK/TiO_2–NC–15	1.81	0.066	8.18	8.07
SPEEK/TiO_2–NC–20	1.73	0.057	7.30	7.81
SPEEK/TiO_2–N–15	1.65	0.047	8.20	5.73
SPEEK/TiO_2–C–15	1.78	0.071	8.33	8.52
SPEEK/TiO_2–P–15	1.44	0.043	6.59	6.53

[a] The standard deviation was ±4.0%.
[b] The standard deviation was ±5.0%.

chains were consumed to form ionic crosslinking with the $-NH_2$ groups on titania surface. Part of the mobile protons might be "trapped" by reacting with basic $-NH_2$ groups [43] and lost their capability for proton conduction. Therefore, the SPEEK/TiO_2–N hybrid membrane showed lower conductivity than pure SPEEK membrane. Moreover, with the TiO_2–NC content increasing from 5 to 15 wt.%, the proton conductivities of SPEEK/TiO_2–NC membranes increased from 0.056 to 0.066 S cm^{-1}. But when the TiO_2–NC content reached 20 wt.%, a decrease in proton conductivity was observed. It could be deduced that a balance existed between the favorable effect of amino acid groups and the unfavorable effect of dilution. The hybrid membrane doped with 15 wt.% amino-acid-functionalized titania exhibited the highest proton conductivity. Since the TiO_2–P had no proton conveying ability, the proton conductivity of the SPEEK/TiO_2–P membrane was lower than that of the pure SPEEK membrane and quite close to that of the control SPEEK/TiO_2 membrane.

In order to further evaluate the influence of these different functional groups on proton conduction, the activation energy values (E_a) for proton conduction were calculated using Arrhenius equation $\sigma = \sigma_0 \exp(-E_a/RT)$, where σ_0 was the pre-exponential factor, k was the Boltzmann's constant and T was the Kelvin temperature. Herein, we conducted the proton conductivity measurement at the temperatures from 20 to 85 °C under 100% RH and the corresponding Arrhenius plots of SPEEK, SPEEK/TiO_2–N, SPEEK/TiO_2–C and SPEEK/TiO_2–NC membranes were displayed in Fig. 7. The activation energies of the hybrid membranes were all in the range of 17–27 kJ mol^{-1}, which were higher than that for merely vehicle mechanism (0–14 kJ mol^{-1}). This indicated that the Grotthuss mechanism and the vehicle mechanism coexisted in the membranes and the former was relatively predominant [44]. The proton conductivity was greatly enhanced by the presence of grafted hydrophilic functional groups. These groups could not only absorb water molecules, but also act as active sites to donate or accept protons and thus facilitate the proton transport. As shown in Fig. 7(a), it was noteworthy that the proton conductivity of SPEEK/TiO_2–N membrane increased with the increasing temperature more notably than that of the pure SPEEK and SPEEK/TiO_2–C membranes. Such phenomenon could be attributed to the facilitated dissociation of sulfonic acid groups on SPEEK at higher temperatures, thus generating abundant protons. Then the pendent $-NH_2$ groups on the titania spheres surface, which interacted with the sulfonic acid groups to form acid–base pairs, could act as a better 'bridge' to promote proton transfer between sulfonic acid groups of SPEEK [45]. The SPEEK/TiO_2–NC membrane exhibited the highest proton conductivity at elevated temperature. It could be tentatively interpreted as follows. The TiO_2–NC had both proton donors (–COOH) and proton acceptors ($-NH_2$), so it might be less influenced by the variation of dissociation degree of $-SO_3H$ groups. Such buffering effect helped the membrane to maintain its proton conducting ability against the change of operational temperature. In addition, compared with the sulfonic groups which had a strong ability to give protons but a weak ability to accept protons, the amino acid groups on the

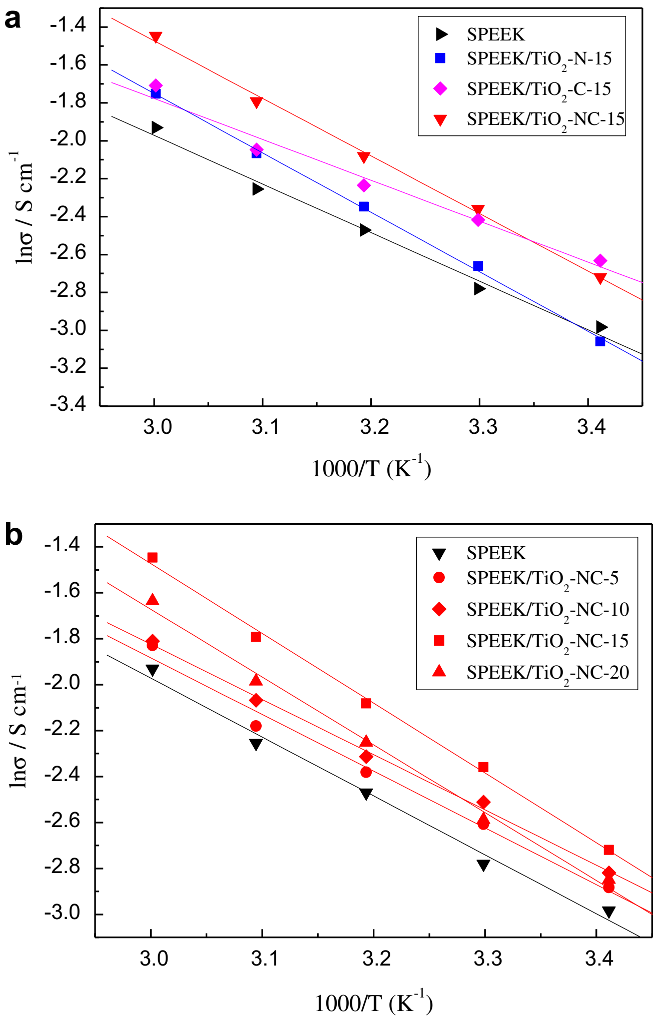

Fig. 7. Proton conductivity of SPEEK and hybrid membranes at different temperatures with various functional fillers (a) and different filler contents (b).

titania surface might ease the proton transport by their dual ability of giving protons and accepting protons. In fact, the proton transport in natural organisms is heavily dependent on the amino acid-lined channels where the amino acids act simultaneously as both proton donors and proton acceptors. In biology, protons mainly transport through hydrophilic proton channels which are formed by transmembrane proteins. The key chemical composition in this channel is an acid–base complex which plays a crucial role in the overall proton transfer through the cell membrane [23–25]. Herein, the lower proton conductivity of SPEEK/TiO_2–N (possessed only the basic amino groups) and SPEEK/TiO_2–C (possessed only the acidic carboxyl groups) membranes than SPEEK/TiO_2–NC membrane further reflected the synergistic and promoting effect of amino acid groups on proton conduction.

3.7. Methanol permeability and selectivity of hybrid membranes

The PEMs with low methanol diffusion coefficient are required for application in DMFCs because the methanol crossover through membrane from anode to cathode will reduce the open-circuit potential and poison the electro catalysts at the cathode. The methanol transport through the membrane is driven by the concentration gradient as well as the electro-osmotic drag between the anode and cathode. It is known that methanol permeated through hydrophilic ionic channels, and so the narrower and more branched hydrophilic channels in SPEEK led to a lower electro-osmotic drag and permeation coefficient compared to Nafion® membrane [46,47]. Herein, the methanol permeability (P, $cm^2\ s^{-1}$) was measured and compared based on diffusion behavior. The methanol permeability of the SPEEK and the hybrid membranes at room temperature was shown in Fig. 8 and the concrete data were presented in Table 1. The methanol permeability of the pristine SPEEK membrane was $11.70 \times 10^{-7}\ cm^2\ s^{-1}$ while the methanol permeability of the hybrid membranes decreased dramatically. As shown in Fig. 8(a), compared to the pristine SPEEK membrane, the methanol permeability decreased monotonically by 18.5–37.6% with increasing content of TiO_2–NC from 5 to 20 wt.%. The titania fillers in the membrane played a key role in suppressing the methanol crossover. On one hand, the inorganic fillers in membrane acted as a methanol barrier by suppressing polymer chain mobility so as to reduce the size of channels for methanol permeation [9]. On the other hand, the existence of inorganic fillers increased the length and tortuosity of methanol diffusion pathways. As displayed in Fig. 8(b), the SPEEK/TiO_2–P–15 membrane showed the lowest methanol permeability of about $6.53 \times 10^{-7}\ cm^2\ s^{-1}$, nearly half of the pure SPEEK membrane. The hydrophobic phenyl groups grafted on the titania surface further suppressed the methanol transport.

The overall performance of the membranes for potential application in DMFC was often preliminarily evaluated by the ratio of proton conductivity to the methanol permeability, named as selectivity [48]. The selectivity values of the pristine SPEEK and the hybrid membranes were listed in Table 1. Accordingly, the selectivities of all the hybrid membranes were improved with the introduction of these inorganic fillers. The SPEEK/TiO_2–C and SPEEK/TiO_2–NC membranes with 15 wt.% of carboxyl acid-functionalized and amino acid-functionalized titania fillers had high selectivity values that were about 1.9 and 1.8-fold to that of the pure SPEEK membrane, owing to both increased proton conductivity and reduced methanol permeability. The results indicated that the organic–inorganic hybrid membranes could endow an effective solution to crossover the “trade-off” hurdle between proton conductivity and methanol permeability for polymer membranes [18].

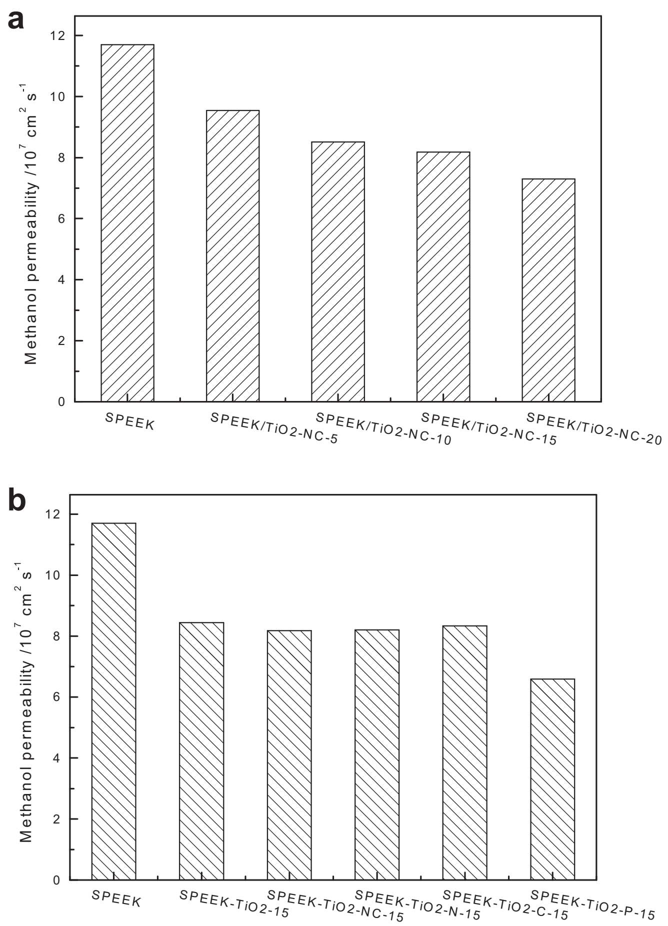

Fig. 8. Methanol permeability of SPEEK and hybrid membranes with various functional fillers (a) and different filler contents (b).

4. Conclusion

In the present study, intrigued by the basic principle of biological energy system, novel amino acid-functionalized titania submicrospheres were successfully synthesized for fabrication of a new type of organic–inorganic hybrid membranes. A series of titania submicrospheres grafted with monofunctional groups including $-NH_2$, $-COOH$ and $-Ph$ were also synthesized and evaluated for comparison purpose. With respect to the proton conductivity, the amino acid based membrane displayed the most desirable performance under intermediate temperature. It was deduced that amino acids containing both proton donor ($-COOH$) and receptor ($-NH_2$) could serve as a good “buffer” against the fluctuation of the surrounding environment so as to act as active sites for proton transfer and thus exerting a favorable effect on proton conductivity. Apart from the improvement in proton conductivity, the hybrid membranes also possessed enhanced thermal stability and reduced methanol permeability. Overall, the amino acid-functionalized hybrid membranes possessed a superior proton conducting ability, showing promising potential as proton exchange membrane materials for DMFC applications under intermediate temperatures.

Acknowledgment

The authors gratefully acknowledge financial support from Program for New Century Excellent Talents in University (NCET-10–0623), the Project-sponsored by SRF for ROCS (Ministry of Education, China), the National Science Fund for Distinguished Young Scholars (21125627), the Programme of Introducing Talents of Discipline to Universities (No. B06006)

References

[1] S.K. Kamarudin, F. Achmad, W.R.W. Daud, Int. J. Hydrogen Energy 34 (2009) 6902–6916.
[2] H. Ahmad, S.K. Kamarudin, U.A. Hasran, W.R.W. Daud, Int. J. Hydrogen Energy 35 (2010) 2160–2175.
[3] K.A. Mauritz, R.B. Moore, Chem. Rev. 104 (2004) 4535–4585.
[4] M.M. Hasani-Sadrabadi, E. Dashtimoghadam, F.S. Majedi, K. Kabiri, J. Power Sources 190 (2009) 318–321.
[5] R.Q. Fu, J.J. Woo, S.J. Seo, J.S. Lee, S.H. Moon, J. Power Sources 179 (2008) 458–466.
[6] R. Gosalawit, S. Chirachanchai, S. Shishatskiy, S.P. Nunes, J. Membr. Sci. 323 (2008) 337–346.
[7] M.L. Di Vona, Z. Ahmed, S. Bellitto, A. Lenci, E. Traversa, S. Licoccia, J. Membr. Sci. 296 (2007) 156–161.
[8] E. Sengul, H. Erdener, R.G. Akay, H. Yucel, N. Bac, I. Eroglu, Int. J. Hydrogen Energy 34 (2009) 4645–4652.
[9] Y.H. Su, Y.L. Liu, D.M. Wang, J.Y. Lai, M.D. Guiver, B.J. Liu, J. Power Sources 194 (2009) 206–213.
[10] V.S. Silva, B. Ruffmann, H. Silva, Y.A. Gallego, A. Mendes, L.M. Madeira, S.P. Nunes, J. Power Sources 140 (2005) 34–40.
[11] J.C. McKeen, Y.S. Yan, M.E. Davis, Chem. Mater. 20 (2008) 5122–5124.
[12] T. Fu, Z. Cui, S. Zhong, Y. Shi, C. Zhao, G. Zhang, K. Shao, H. Na, W. Xing, J. Power Sources 185 (2008) 32–39.
[13] R. Kannan, B.A. Kakade, V.K. Pillai, Angew. Chem. Int. Ed. 47 (2008) 2653–2656.
[14] Y.-H. Su, Y.-L. Liu, Y.-M. Sun, J.-Y. Lai, D.-M. Wang, Y. Gao, B. Liu, M.D. Guiver, J. Membr. Sci. 296 (2007) 21–28.
[15] M. Nogami, T. Mitsuoka, K. Hattori, Y. Daiko, Microporous Mesoporous Mater. 86 (2005) 349–353.
[16] H. Wu, W. Hou, J. Wang, L. Xiao, Z. Jiang, J. Power Sources 195 (2010) 4104–4113.
[17] C.A. Alabi, M.E. Davis, Chem. Mater. (a) 18 (2006) 5634–5636.
[18] T. Xu, W. Hou, X. Shen, H. Wu, X. Li, J. Wang, Z. Jiang, J. Power Sources 196 (2011) 4934–4942.
[19] Y. Xue, R. Fu, C. Wu, J.Y. Lee, T. Xu, J. Membr. Sci. 350 (2010) 148–153.
[20] W.F. Chen, J.S. Wu, P.L. Kuo, Chem. Mater. 20 (2008) 5756–5767.
[21] A. Carbone, R. Pedicini, A. Saccà, I. Gatto, E. Passalacqua, J. Power Sources 178 (2008) 661–666.
[22] S.R. Benhabbour, R.P. Chapman, G. Scharfenberger, W.H. Meyer, G.R. Goward, Chem. Mater. 17 (2005) 1605–1612.
[23] I. Bento, P.M. Matias, A.M. Baptista, P.N. da Costa, W.M.A.M. van Dongen, L.M. Saraiva, T.R. Schneider, C.M. Soares, M.A. Carrondo, Proteins 54 (2004) 135–152.
[24] M. Shibata, H. Yamashita, T. Uchihashi, H. Kandori, T. Ando, Nat. Nanotechnol. 5 (2010) 208–212.
[25] H. Tributsch, L. Pohlmann, J. Theor. Biol. 178 (1996) 17–28.
[26] H.J. Leem, I. Dorbandt, J. Rojas-Chapana, S. Fiechter, H. Tributsch, J. Phys. Chem. C 112 (2008) 2756–2763.
[27] A. Statz, J. Finlay, J. Dalsin, M. Callow, J.A. Callow, P.B. Messersmith, Biofouling: J. Bioadhesion Biofilm Res. 22 (2006) 391–399.
[28] R. Rodríguez, M.A. Blesa, A.E. Regazzoni, J. Colloid Interface Sci. 177 (1996) 122–131.
[29] G.-L. Wang, J.-J. Xu, H.-Y. Chen, Biosens. Bioelectron. 24 (2009) 2494–2498.
[30] G. Kim, L.Y. Hong, J. Jung, D.P. Kim, H. Kim, I.J. Kim, J.R. Kim, M. Ree, Biomaterials 31 (2010) 2517–2525.
[31] P.X. Xing, G.P. Robertson, M.D. Guiver, S.D. Mikhailenko, K.P. Wang, S. Kaliaguine, J. Membr. Sci. 229 (2004) 95–106.
[32] L. Li, J. Zhang, Y.X. Wang, J. Membr. Sci. 226 (2003) 159–167.
[33] X.C. Jiang, T. Herricks, Y.N. Xia, Adv. Mater. 15 (2003) 1205–1209.
[34] A.F. Ismail, N.H. Othman, A. Mustafa, J. Membr. Sci. 329 (2009) 18–29.
[35] M.L. Di Vona, E. Sgreccia, A. Donnadio, M. Casciola, J.F. Chailan, G. Auer, P. Knauth, J. Membr. Sci. 369 (2011) 536–544.
[36] C.J. Zhao, H.D. Lin, K. Shao, X.F. Li, H.Z. Ni, Z. Wang, H. Na, J. Power Sources 162 (2006) 1003–1009.
[37] H.T. Li, Z.M. Cui, C.J. Zhao, J. Wu, T.Z. Fu, Y. Zhang, K. Shao, H.Q. Zhang, H. Na, W. Xing, J. Membr. Sci. 343 (2009) 164–170.
[38] N. Hara, H. Ohashi, T. Ito, T. Yamaguchi, J. Phys. Chem. B 113 (2009) 4656–4663.
[39] K.-D. Kreuer, Chem. Mater. 8 (1996) 610–641.
[40] J. Wang, H. Zhang, Z. Jiang, X. Yang, L. Xiao, J. Power Sources 188 (2009) 64–74.
[41] D.S. Kim, B. Liu, M.D. Guiver, Polymer 47 (2006) 7871–7880.
[42] M. Schuster, T. Rager, A. Noda, K.D. Kreuer, J. Maier, Fuel Cells 5 (2005) 355–365.
[43] X. Li, E.P.L. Roberts, S.M. Holmes, V. Zholobenko, Solid State Ionics 178 (2007) 1248–1255.
[44] B. Smitha, S. Sridhar, A.A. Khan, Macromolecules 37 (2004) 2233–2239.
[45] Y.Z. Fu, A. Manthiram, M.D. Guiver, Electrochem. Commun. 9 (2007) 905–910.
[46] M. Ise, K.D. Kreuer, J. Maier, Solid State Ionics 125 (1999) 213–223.
[47] K.D. Kreuer, J. Membr. Sci. 185 (2001) 29–39.
[48] J. Zhu, G. Zhang, K. Shao, C. Zhao, H. Li, Y. Zhang, M. Han, H. Lin, M. Li, H. Na, J. Power Sources 196 (2011) 5803–5810.